Review | Received 9 May 2026; Revised 30 June 2026; Accepted 21 July 2026; Published 21 August 2026
https://doi.org/10.55092/bi20260002

The application of artificial intelligence-driven generative design and bioinformatics modeling in tissue engineering scaffolds

Hao Deng[1], Zheng Qin[2,*] and Mingru Kong[1,2,3,*]

[1] Nanshan School, Guangzhou Medical University, Guangzhou, China
[2] Guangzhou Women and Children's Medical Center, Guangzhou, China
[3] Department of Anatomy, School of Basic Medical Sciences, Guangzhou Medical University, Guangzhou, China

* Correspondence authors; E-mails: qinzheng@emails.imau.edu.cn (Z.Q.); kongmingru@gzhmu.edu.cn (M.K.).

Highlights:

- Explores how generative AI and bioinformatics can inform the design of tissue-specific scaffolds.
- Discusses the use of multimodal scaffold data to support biologically guided inverse design.
- Reviews current generative models, validation challenges, and barriers to clinical translation.

Abstract: The architecture of a tissue-engineering scaffold affects how cells attach, migrate, and remodel newly formed tissue. At present, many scaffolds are still developed through repeated adjustment of a few structural variables, making it difficult to balance porosity with mechanical strength or degradation with the pace of tissue formation. Generative artificial intelligence may help shift scaffold development toward a target-driven process. Given a desired biological or mechanical outcome, a model could identify structures that are likely to achieve it. This possibility depends on training data that connect scaffold features with biological responses. In this review, we consider the use of generative methods together with bioinformatics for scaffold design. We describe potentially useful data sources, including micro-computed tomography (CT) images, mechanical measurements, single-cell RNA sequencing, and degradation data. We also examine generative adversarial networks, variational autoencoders, diffusion models, and evolutionary algorithms. Rather than treating these approaches as interchangeable, we discuss the design tasks for which their strengths differ. Examples from cardiac, bone, cartilage, and related applications show how tissue context shapes data requirements and model selection. We close by considering data comparability, validation across length scales, and the practical challenges of clinical use. These issues will determine whether generative tools can support more tailored scaffold design.

Keywords: tissue engineering; tissue scaffolds; generative artificial intelligence; bioinformatics; regenerative medicine

1. Introduction

Tissue engineering seeks to restore damaged tissues by developing functional biological substitutes. In this context, scaffolds are commonly used as temporary three-dimensional matrices that provide structural support during regeneration. Their architecture and material properties influence the local conditions for cell attachment, proliferation, and differentiation [1]. Despite substantial progress in scaffold fabrication, design still relies heavily on experimental iteration. It remains difficult to reconcile competing requirements, such as high porosity and adequate mechanical strength, or scaffold degradation and the pace of tissue formation [2]. Computer-aided methods, including finite element analysis, can integrate multiple inputs and predict aspects of scaffold behaviour. Their use remains limited by complex geometries and simplified physiological representations [3,4].

Supervised models estimate scaffold performance from structural and material variables, whereas inverse-design models generate candidates for defined targets [5–7]. Surrogate models can be coupled with evolutionary search [8,9]. Their value depends on the target, available data, and tissue context [10,11]. Training data should link structure to mechanical, imaging, cellular, molecular, and degradation outcomes [12,13]. Most reports examine one tissue setting, leaving limited guidance for adapting computational strategies across tissues [14–16]. This review compares generative design and bioinformatics across tissue contexts, focusing on data requirements, validation, and clinical translation.

2. Multimodal biological information required for the design of the support structure

Generative inverse design depends on compatible training data [17]. Micro-CT captures architecture but not cell behaviour, whereas omics data reveal biological responses without establishing mechanical competence. Useful datasets should combine morphology, mechanics, biological outcomes, and degradation behaviour [18].

2.1. Morphological imaging information

Imaging data are commonly used to convert scaffold architecture into variables that can be analysed quantitatively. Micro-computed tomography (micro-CT) is particularly useful because it provides three-dimensional information without damaging the sample. Depending on the scanning conditions, resolutions of approximately 1–50 µm can be obtained. Micro-CT can therefore be used to measure porosity, pore-size distribution, specific surface area, and pore connectivity [19,20]. The reconstructed voxel data can be used either as model inputs or as the starting geometry for finite element method (FEM) simulations. Imaging can also be used to follow scaffold changes over time. Schädli *et al.* used time-lapsed micro-CT combined with image registration to monitor local mineral formation in cell-seeded nanocomposite scaffolds under static and dynamic culture conditions [21] (Figure 1A). Color-coded cross-sectional images enabled visualization of spatial changes in mineral formation, while the corresponding image-based analysis quantified mineral formation and resorption volumes over time. These measurements provide quantitative information on how scaffold-associated mineralization changes with time. In another study, porosity was varied from 20% to 90%, giving approximately 14-fold and 9-fold changes in Young's modulus and compressive strength, respectively [22]. Thus, image-derived structural variables can be related to mechanical measurements. The main limitation is that few publicly

available datasets contain both scaffold images and experimentally measured mechanical properties. Simulated micro-CT datasets are consequently still used in many studies [23]. This can be problematic because models trained on a small number of samples may not transfer well to other scaffold geometries or material systems.

SEM is generally used when finer details of fibrous scaffolds are required. For electrospun constructs, fibre diameter, orientation, and packing density can be measured directly from SEM images. These features were used as inputs in a study of 2214 electrospun scaffold samples, in which 12 machine-learning methods were compared for predicting tensile strength and Young's modulus. Confocal microscopy shows cell distribution within three-dimensional scaffolds. In Hilbert microcapillary scaffolds, neural stem cells aligned with capillary membranes and formed networks [24]. Such observations are relevant when structural features are considered together with cell behaviour.

Several studies have attempted to predict mechanical properties directly from imaging data. Three-dimensional CNNs can estimate properties from tomographic images [7]. Coefficients of determination were above 0.90 for Gyroid, Schwarz-P, and Diamond geometries. The performance depends on the quality and diversity of paired experimental data [25]. Taken together, these studies show that imaging data can support property prediction, but their reliability still depends on the quality and diversity of the accompanying experimental data.

2.2. Mechanical characterization data

Mechanical characterization provides the labels needed to train models that predict scaffold performance. Nanoindentation, uniaxial or biaxial compression tests, dynamic mechanical analysis (DMA), and rheological measurements can generate stress–strain curves, elastic moduli, and viscoelastic parameters [26]. These measurements can then be paired with structural or processing variables during model development.

Ibrahimi *et al.* assembled a dataset containing more than 1000 TPMS scaffolds. The scaffolds were characterized using finite element modelling and image analysis before machine-learning models were trained. The nonlinear models reported a median error below 3% and a coefficient of determination above 0.89 [27] (Figure 1B). The models were used to predict scaffold parameters while considering biomechanical, mechanobiological, and manufacturing constraints. Recent work has also moved beyond predictions based only on elastic properties. Model-free approaches can use frequency-domain data from DMA and nanoindentation directly, allowing viscoelastic behaviour to be included without first fitting a constitutive equation [28].

2.3. Cellular and molecular omics data

Cellular and molecular omics data provide information about scaffold-associated biological responses at the level of gene expression [29]. Their use in generative scaffold design is not straightforward, however, because transcriptomic datasets are high-dimensional and require conversion into representations that can be processed by computational models.

Single-cell RNA sequencing (scRNA-seq) measures gene-expression profiles for individual cells. Several approaches can be used to represent these data. One approach is to reduce gene-expression profiles to latent variables. Variational autoencoders, such as single-cell Variational Inference (scVI), can learn low-dimensional representations of cellular states that may be used as conditional inputs for generative adversarial networks or diffusion models [30]. A second approach uses cell annotations, such

as cell type or state, as embedding vectors that condition the model during generation [31]. A third approach infers gene regulatory networks from scRNA-seq data and uses these networks as prior constraints [32]. In this way, count matrices can be converted into latent embeddings, cell labels, or network-based masks for subsequent modelling.

Spatial transcriptomics adds information about where gene-expression patterns occur in a tissue [33]. Spatial data can be represented as graphs, in which cells are treated as nodes and physical proximity defines the edges. Graph neural networks can then process both spatial relationships and gene-expression features. For example, Celcomen uses generative graph neural networks to separate intra- and intercellular gene-regulation programmes [34]. The resulting spatially informed representations may be useful when scaffold design aims to reproduce aspects of native tissue organization.

Several studies have used single-cell or spatial transcriptomics to examine scaffold-related biological responses. scRNA-seq has identified skeletal stem-cell subpopulations with high chondrogenic potential and informed the functionalization of three-dimensionally printed hydrogel scaffolds [35]. In a multi-enzymatic hydrogel scaffold, scRNA-seq was also used to investigate how nitric oxide and reactive oxygen species affect macrophage repolarization in a diabetic microenvironment [36]. After extracellular matrix (ECM) scaffold implantation, combined scRNA-seq and spatial transcriptomics identified macrophage subpopulations that differed in both function and location [37]. Similarly, a Xenium-based spatial-transcriptomics study of a subcutaneous PCL scaffold model identified distinct macrophage and fibroblast populations in separate spatial regions [38] (Figure 1C). These studies provide candidate biological outcomes that can be considered when defining scaffold-design objectives.

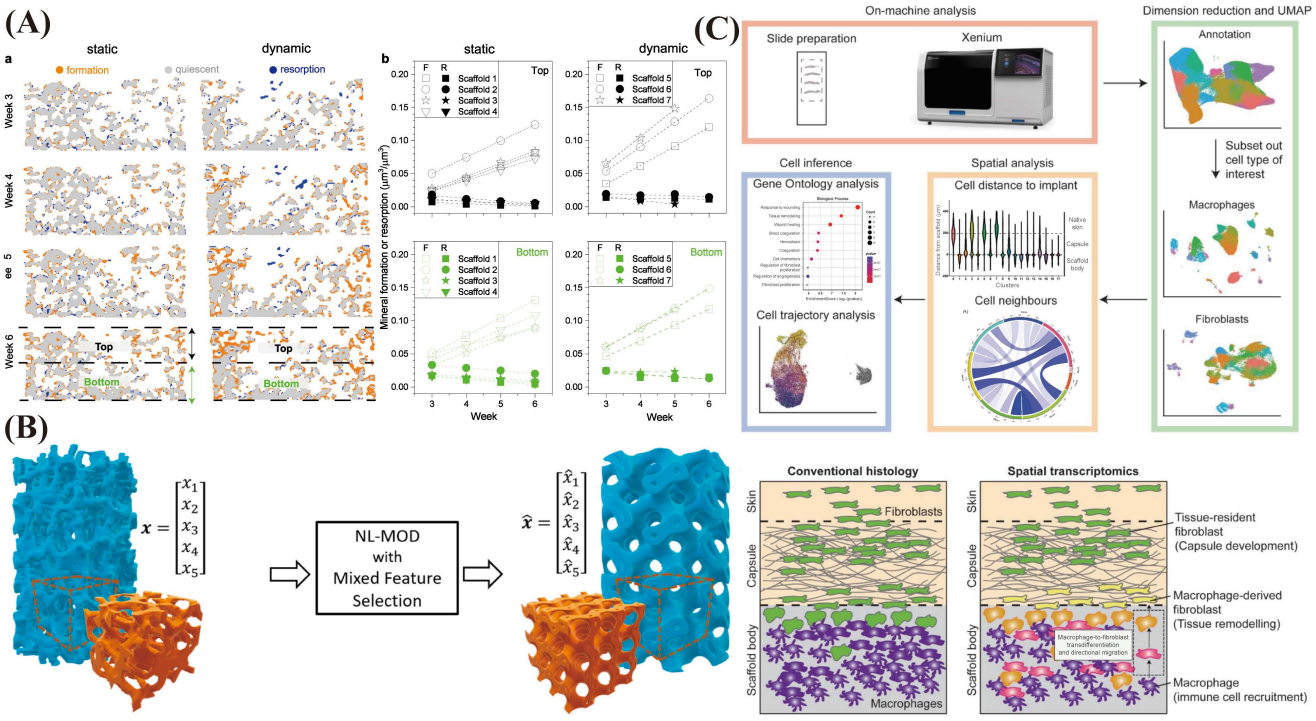

Figure 1. Multimodal data sources for AI-driven scaffold design. **(A)** Time-lapsed micro-CT monitoring and local mineral formation analysis of cell-seeded nanocomposite scaffolds. **(a)** Color-coded cross-sectional micro-CT images of static and dynamically cultured HA55-PLGA (u) scaffolds after 3, 4, 5, and 6 weeks, showing mineral formation (orange), regions classified as resorption (blue), and quiescent regions (gray). **(b)** Mineral formation and resorption volumes

quantified from registered micro-CT images and normalized to the analyzed scaffold volume over time [21]; **(B)** Nonlinear machine learning framework (NL-MOD) mapping microstructural feature vectors extracted from trabecular-like scaffold representative volume elements to predicted mechanical and morphological properties of target TPMS-based scaffolds, enabling prescriptive inverse design without iterative finite element analysis [27]; **(C)** Xenium-based spatial transcriptomics pipeline for *in vivo* scaffold evaluation, integrating on-machine analysis, uniform manifold approximation and projection (UMAP)-based cell annotation, and spatial inference to resolve transcriptionally and spatially distinct macrophage and fibroblast subpopulations across the polycaprolactone (PCL) scaffold microenvironment, providing mechanistic evidence for geometry-driven cellular responses beyond conventional histological resolution [38]. This figure is licensed under the Creative Commons Attribution 4.0 International License (CC BY 4.0).

A remaining challenge is to translate omics measurements into design-relevant constraints. In practice, this involves identifying relevant cell types, cell states, or spatial patterns; defining the biological outcome of interest; and incorporating that outcome into a model. The targets may be encoded as conditional variables, loss-function terms, or regularization terms [39,40]. For example, a bone scaffold might be assessed for its ability to support selected osteogenic cell populations, whereas a cardiac scaffold might be designed to promote an appropriate spatial arrangement of cardiomyocytes and fibroblasts. MORPHE has shown that spatial-omics data can be represented in continuous latent spaces that are compatible with diffusion models. Such approaches offer a route from descriptive omics data to explicit biological criteria for scaffold design (Figure 2).

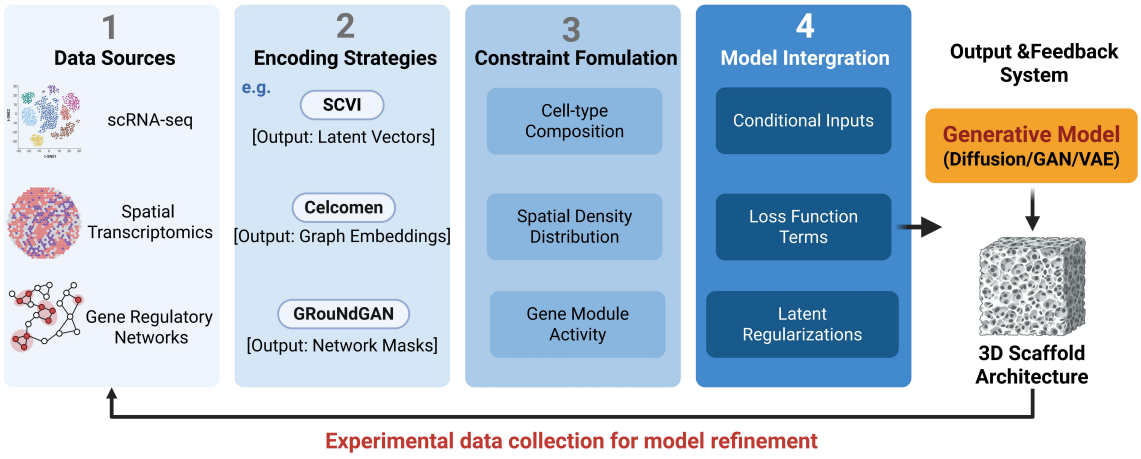

Figure 2. Schematic pipeline for encoding omics data into generative scaffold design. scRNA-seq and spatial transcriptomics data are encoded through VAE-based (scVI, scGEN), graph neural network-based (Celcomen, SPATIA), or network-guided (GRouNdGAN) strategies into structured representations—latent vectors, graph embeddings, and network masks, respectively [31,41]. These representations are then formulated into design-relevant biological constraints, including cell-type composition, spatial density distribution, and gene module activity [39,40]. These constraints are subsequently embedded into generative models through three routes: as conditional inputs, loss function terms, or latent-space regularizations [42]. The constrained generative model outputs 3D scaffold architectures, with experimental data informing model refinement in a feedback loop [38]. Literature references for each encoding strategy and integration approach are indicated in brackets. This figure was created using https://www.biorender.com/.

A biomaterial-mediated cell atlas may organize links between material properties and transcriptional responses [43]. Single-cell and spatial-transcriptomic studies are beginning to clarify how scaffold properties affect cell behaviour [38]. Single-cell and spatial-transcriptomic studies suggest that stiffness and topography can alter YAP/TAZ activity through RhoA/ROCK signalling and cytoskeletal dynamics, with consequences for proliferation, differentiation, and immune polarization [44]. Chiral hydroxyapatite-gradient scaffolds, for example, promoted osteochondral regeneration while altering stress-fibre distribution and YAP nuclear transport in bone-marrow stromal cells [45]. Single-cell studies describe immune remodelling after implantation, including macrophage recruitment and polarization [46]. Other studies have observed cell-state changes after scaffold implantation, including shifts between stem-cell states and the emergence of progenitor-like features in differentiated cells [47]. These findings provide mechanistic context for selecting biological outcomes in scaffold design.

2.4. Degradation kinetics and biocompatibility data

Degradation and biocompatibility data are needed to evaluate whether a scaffold remains suitable during tissue regeneration. Relevant measurements include degradation rate, cell viability, proliferation, and cytokine secretion. When paired with processing and structural variables, these measurements can be used to train models of degradation behaviour and biological compatibility.

Das *et al.* combined an artificial neural network with a genetic algorithm to relate fabrication variables to alginate-gel scaffold properties. Using viscosity, surface tension, and contact angle as inputs, the model predicted scaffold porosity with a maximum deviation of 3.7% from the experimental values [48]. Similar mapping approaches have linked processing parameters with several scaffold properties and could be adapted for models of degradation or biocompatibility [25]. In a rat skin-defect model, artificial neural network (ANN)-optimized electrospun scaffolds promoted wound closure and tissue regeneration, extending the evaluation from *in vitro* structural properties to *in vivo* outcomes [49].

Degradation modelling can also incorporate information from material libraries. A physics-constrained deep reinforcement-learning framework used high-throughput synthesis and characterization data from 847 polymers to identify degradation profiles for several material classes over 6–24 months [50]. This type of framework may help include degradation behaviour in predictive or generative scaffold models. Overall, well-annotated degradation and biocompatibility datasets are needed if scaffold models are to be assessed against biological performance rather than structural properties alone.

3. Core generative and optimization-driven approaches

3.1. Generative adversarial networks

Generative adversarial networks (GANs) learn to generate new samples through the interaction of a generator and a discriminator. They have been widely used to reconstruct and generate porous architectures, including three-dimensional scaffold geometries. In voxel-based representations, GANs can generate internal pore networks and interconnected channels with considerable structural complexity. Some studies have reported porosity errors within 1% of the corresponding reference samples [51,52].

Conditional GANs can incorporate target properties during generation. For example, a three-dimensional conditional GAN was trained using 10,000 Voronoi lattice structures with associated relative-density

and Young's-modulus data. The generated structures were evaluated by uniaxial compression tests and finite element simulations. This model produced candidate bone-scaffold architectures with prescribed porosity and stiffness [8] (Figure 3A). However, GAN training can be unstable, particularly when the available dataset is small. Model collapse can reduce architectural diversity, whereas greater diversity can compromise physical feasibility [53]. Transferability is a separate challenge.

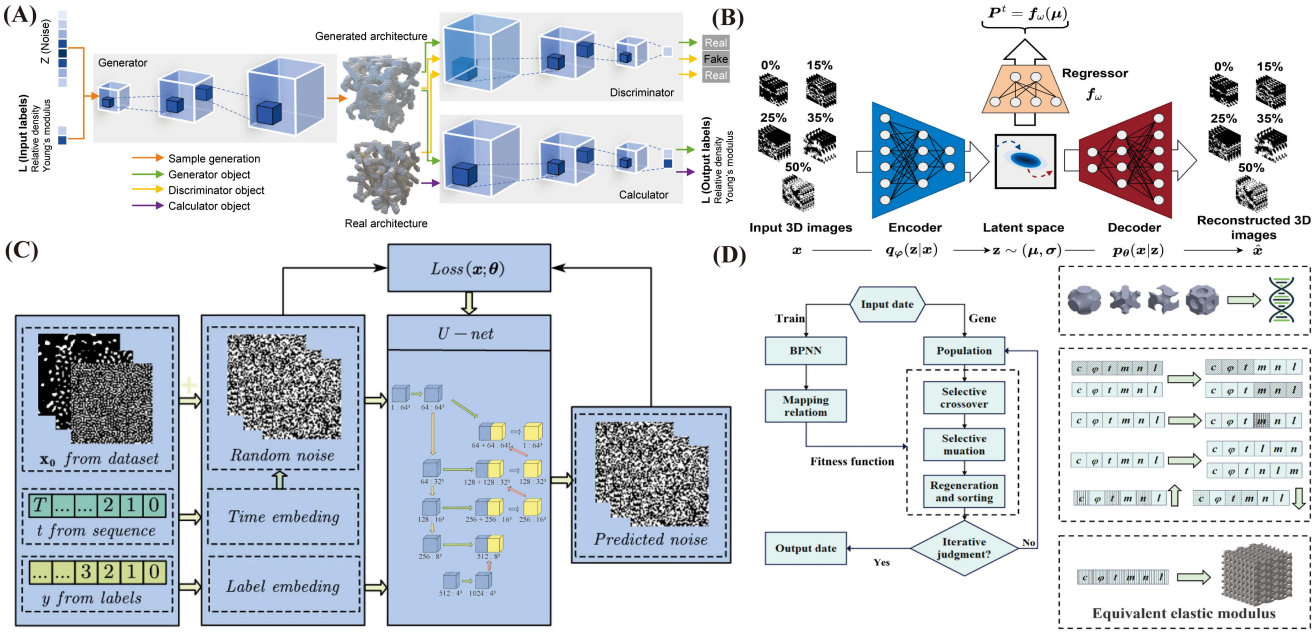

Figure 3. Representative generative and optimization approaches for scaffold inverse design. **(A)** A three-dimensional conditional GAN (3D-CGAN) uses generator, discriminator, and calculator modules to generate Voronoi bone scaffolds with target relative density, porosity, and Young's modulus [8]; **(B)** In a property-augmented variational autoencoder (pVAE), the encoder maps 3D porous microstructures to a latent distribution, the regressor predicts target properties, and the decoder reconstructs the microstructure for gradient-based inverse design [54]; **(C)** A conditional denoising diffusion probabilistic model (DDPM) combines time and label embeddings with a U-Net denoising backbone to generate label-conditioned microstructures [9]; **(D)** Regenerative genetic algorithm used for inverse scaffold design. Candidate TPMS structures are evaluated according to their predicted mechanical properties and updated through selection, crossover, mutation, and regeneration until a suitable solution is obtained [11]. This figure is licensed under the Creative Commons Attribution 4.0 International License (CC BY 4.0).

3.2. Variational autoencoders

Variational autoencoders (VAEs) represent scaffold structures in a lower-dimensional latent space. This representation can be useful for exploring relationships between structural features and performance. When a VAE is combined with a regression model, latent variables can be associated with mechanical properties. Such VAE-regression frameworks can support both forward prediction, from structure to performance, and inverse design, from a target property to a candidate structure [55].

Conditional VAEs provide an additional way to include target properties during generation. In these models, property values are introduced as conditions when latent variables are sampled or optimized. A

regressor-augmented VAE, termed pVAE, was used to design porous metamaterials with target porosity and permeability. The approach was evaluated using synthetic data and computed-tomography scans of real foams [54] (Figure 3B). The continuity of the latent space can also be used to generate gradual changes in microstructure. For example, spherical linear interpolation (SLERP) between latent codes can produce a sequence of related structures. This may be useful for designing graded scaffolds, such as those intended to mimic transitions between bone and cartilage [56].

VAEs also have limitations. Their output quality depends on how well the latent space represents the training data. In hybrid VAE-GAN models, reconstruction of three-dimensional stochastic structures from two-dimensional images has been associated with deviations in both mechanical and morphological properties [57]. This issue is particularly relevant when scaffold performance depends strongly on three-dimensional connectivity or anisotropy.

3.3. Diffusion models

Diffusion models generate samples by gradually removing noise from an initially random representation. They have been applied to the reconstruction of two- and three-dimensional material microstructures. Compared with GANs, diffusion models are often easier to train and may produce more diverse samples, although their performance depends on the dataset, conditioning strategy, and evaluation criteria [58]. Denoising diffusion probabilistic models have been used for microstructure reconstruction in several composite-material systems. Denoising diffusion implicit models (DDIMs) have also been used to generate graded materials through interpolation in the latent space [9] (Figure 3C).

Diffusion models can incorporate more than one input modality. The multimodal-guided latent diffusion model (MG-LDM), for example, used stress–strain data, stress fields, and printing parameters to guide the design of skin tissue-engineering scaffolds. In the reported study, the method outperformed the selected baseline models [18]. At present, the main practical limitation of diffusion models is sampling cost. Generating a structure usually requires multiple denoising steps, which can increase computation time relative to single-pass generative models.

3.4. Evolutionary algorithms

Evolutionary algorithms (EAs) differ from GANs, VAEs, and diffusion models because they do not learn a probability distribution of scaffold structures. Instead, they search a design space by repeatedly evaluating and updating a population of candidate solutions. GAs and particle swarm optimization (PSO) are commonly used examples. These methods are useful when design variables are discrete, the objective is multimodal, or gradients are unavailable. In scaffold optimization, structural parameters are treated as candidate solutions, and mechanical responses predicted by finite element analysis or surrogate models serve as fitness criteria. Selection, crossover, and mutation then update the population. Liu *et al.* coupled a BPNN with a regenerative genetic algorithm (RGA). The BPNN predicted the relationship between TPMS parameters and equivalent stiffness matrices, while the RGA searched for structures satisfying target-stiffness constraints (Figure 3D). The mean error across three mechanical metrics was below 3% [11].

A related BPNN-GA framework was applied to spinodoid bone scaffolds. In that study, the anisotropic elastic matrix of target bone tissue was used as the optimization objective. The generated

structures showed close agreement with the target mechanical properties along three orthogonal directions [10] . PSO-based neural-network frameworks have also been used to optimize dendritic fractal bone scaffolds while considering both yield strength and elastic modulus [59]. In these hybrid approaches, surrogate models reduce the cost of repeatedly evaluating candidate structures, whereas evolutionary algorithms perform the search. Their efficiency can still decrease as the number of design variables and population size increase. Table 1 summarizes the representative methods discussed in this section.

Table 1. Summary of representative AI-based scaffold design methods and their validation status.

Method Category	Specific Approach	Data Modality	Tissue or Biological Context	Key Reported Metric	Validation Level	References
Hybrid	Topology optimization with self-supporting constraints	Process parameters	General additive manufacturing	Overhang angle and length constraints	In silico	[60]
Hybrid	Transfer learning with GA-BPNN and PSO	TPMS structural parameters	Bone TPMS scaffolds	Avg error 7.6% for PCU, 4.8% for Ti alloy	In silico and experimental	[12]
Surrogate	ML: RF, SVR, K-NN, GBR	FFF process parameters	Bone FFF scaffolds	> 99% prediction accuracy	*In vitro*	[61]
Surrogate with validation	ANN-optimized electrospun scaffold	PCL/PEG electrospun parameters	Rat skin wound healing	Neovascularization and wound closure	*In vitro* and *in vivo*	[49]
Generative with validation	GAN with active learning	Multimodal: transcription, imaging, biomechanical	Bone tissue engineering	SSIM 0.89, ICC 0.81	In silico	[62]
Generative	Celcomen, a generative GNN	Spatial transcriptomics	General spatial biology	Spatial causal disentanglement	In silico	[34]
Generative	SPATIA with hierarchical attention	Morphology, gene expression, spatial coordinates	Spatial cell phenotypes	Spatially aware latent representations	In silico	[41]
Generative	TriTopo-LGDM	Trabecular bone histology	Trabecular bone scaffolds	Morphological and mechanical matching	In silico	[42]
Surrogate	3D CNN	Virtual tomographic images	Bone TPMS scaffolds	$R^2 > 0.90$ for elastic modulus and permeability	In silico	[7]
Surrogate	Nonlinear ML	FEM and image analysis	Trabecular bone scaffolds	Median error < 3%, $R^2 > 0.89$	In silico	[27]
Biological constraint	scRNA-seq with 3D-printed scaffold	Single-cell transcriptomics	Osteochondral stem cell differentiation	Chondrogenic stem cell identification	*In vitro* and *in vivo*	[35]
Biological validation	Xenium spatial transcriptomics	Spatial transcriptomics	PCL scaffold in mouse model	Macrophage and fibroblast subpopulations	*In vivo*	[38]
Surrogate	ANN-GA	Alginate gel fabrication parameters	Soft tissue alginate scaffolds	Porosity prediction with max deviation 3.7%	*In vitro*	[48]
Generative	3D-CGAN	Voronoi lattice structures	Bone Voronoi scaffolds	Porosity and stiffness control	In silico	[8]

Table 1. *Cont.*

Method Category	Specific Approach	Data Modality	Tissue or Biological Context	Key Reported Metric	Validation Level	References
Generative	VAE-Regression	Microstructural images	General microstructure design	Forward prediction and inverse inference	In silico	[55]
Generative	DDPM and DDIM	2D and 3D composite microstructures	Composite material design	High-fidelity microstructure reconstruction	In silico	[9]
Hybrid	BPNN with RGA	TPMS structural parameters	Bone TPMS scaffolds	Mean error < 3% across three metrics	In silico	[11]
Hybrid	BPNN with GA	Spinodoid scaffold parameters	Spinodoid bone scaffolds	Anisotropic elastic matrix matching	In silico	[10]
Hybrid	PSO with BP-NSGA-III	Dendritic fractal scaffold parameters	Dendritic fractal bone scaffolds	Yield strength and elastic modulus	In silico	[59]
Generative with validation	Topology optimization and 3D printing	PCL scaffold parameters	Cardiac PCL patches	Cardiomyocyte infiltration and hemodynamic stability	*In vitro* and *in vivo*	[63]
Surrogate	Multinomial logistic regression	Polymer database	Cartilage polymer blends	Optimal polymer blend prediction	In silico	[64]
Hybrid	Direct MultiSearch optimization	TPMS scaffold parameters	Bone and cartilage TPMS scaffolds	Pareto-optimal mechanical and transport performance	In silico	[65]

Studies are organized by method category, specific approach, data modality, tissue or biological context, validation level, and key reported metrics. Method categories include generative inverse design, which directly learns inverse mappings from performance to structure; surrogate or forward models, which predict performance from structure without generating new designs; hybrid approaches combining surrogate models with evolutionary or optimization algorithms; biological constraint studies that use omics data to inform generative model constraints; and biological validation studies that employ omics techniques to evaluate scaffold performance *in vivo*. Validation levels are classified as in silico (computational validation only), *in vitro* (laboratory experiments with cells or tissues), or *in vivo* (animal model validation). "General" denotes methods developed for broader applicability across tissue types. Literature references are indicated in brackets. Abbreviations: 3D-CGAN: three-dimensional conditional generative adversarial network; ANN: artificial neural network; BPNN: back-propagation neural network; CNN: convolutional neural network; DDIM: denoising diffusion implicit model; DDPM: denoising diffusion probabilistic model; FEM: finite element method; FFF: fused filament fabrication; GA: genetic algorithm; GAN: generative adversarial network; GBR: gradient boosting regression; GNN: graph neural network; ICC: intraclass correlation coefficient; K-NN: K-nearest neighbors; LGDM: latent graph diffusion model; ML: machine learning; NSGA-III: nondominated sorting genetic algorithm III; PCL: polycaprolactone; PCU: polycarbonate urethane; PEG: polyethylene glycol; PSO: particle swarm optimization; RF: random forest; RGA: regenerative genetic algorithm; scRNA-seq: single-cell RNA sequencing; SPATIA: multimodal generation and prediction of spatial cell phenotypes; SSIM: structural similarity index measure; SVR: support vector regression; TPMS: triply periodic minimal surface; VAE: variational autoencoder.

4. Applications of AI-generated scaffolds

4.1. Cardiac tissue engineering scaffolds

Cardiac scaffolds must address several features of native myocardium. Myocardial tissue has an anisotropic extracellular matrix, nonlinear mechanical behaviour, and coordinated electrical activity. Scaffold design therefore needs to consider fibre orientation, mechanical compatibility with the surrounding tissue, and support for electrical conduction [66]. Current computational approaches address these requirements to different extents rather than modelling all of them simultaneously.

Mechanical surrogate models have been used to support the design of cardiac patches. Random-forest and response-surface models, for example, have been used to estimate design parameters from target mechanical properties. In the reported studies, the resulting designs were assessed by compression testing, suggesting that such models may be useful for mechanically tailored scaffold development [67]. Topology optimization has also been applied to cardiac scaffolds. One study used anisotropic mechanical objectives to design PCL metamaterial scaffolds. Following volumetric three-dimensional printing, the scaffolds supported cardiomyocyte infiltration and contraction *in vitro*. The same study also reported that the constructs tolerated intraventricular pressure and improved hemodynamic stability in a large-animal myocardial-defect model [63].

Not all artificial-intelligence applications in cardiac engineering directly generate scaffolds. Generative adversarial networks, for instance, have been used to create synthetic cardiomyocyte images for training classifiers of cellular maturity [68]. This application may improve the throughput of cell-response assessment, but it does not itself establish a scaffold-design workflow. Similarly, an incompressible orthotropic constitutive neural network was used to identify constitutive forms and parameters for human cardiac tissue from a large candidate set [69] (Figure 4A). Such models may provide more realistic mechanical inputs for scaffold design, although further work is required to connect them with scaffold-generation methods.

The main limitation is the lack of integrated datasets for cardiac scaffolds. Data describing fibre orientation, nonlinear mechanics, electrical conduction, and long-term cyclic loading are rarely available in the same dataset. In addition, many computational designs have been assessed mainly by simulation or short-term testing. Their fatigue resistance and structural stability under ventricular loading remain insufficiently characterized. Future studies should evaluate generated designs under cyclic loading and include electrophysiological outcomes, contractile synchrony, and mechanical integrity as separate validation measures.

4.2. Bone tissue engineering scaffolds

Bone-scaffold design must balance mechanical support against mass transport. Increasing porosity can improve permeability, nutrient delivery, and tissue ingrowth, but usually lowers stiffness and strength. Computational optimization can examine this trade-off more efficiently than repeated finite element simulations alone [4].

Several generative and optimization-based approaches have been reported. The TriTopo-latent graph diffusion model (LGDM) combines topology optimization with a latent graph diffusion model to relate scaffold parameters to target mechanical properties. The generated structures were reported to

have morphological and mechanical characteristics similar to those of cancellous bone [42]. Bio-inspired computational design provides another way to tailor scaffold-like structures to local mechanical requirements. Jia *et al.* developed a generative framework for irregular architected materials, combining a virtual growth model with machine learning to relate local structural patterns to their mechanical properties [70] (Figure 4B). The method was demonstrated in a fractured-femur model, where the distribution of different building blocks was optimized to adjust the stress around the defect. The resulting support structures were subsequently fabricated by 3D printing.

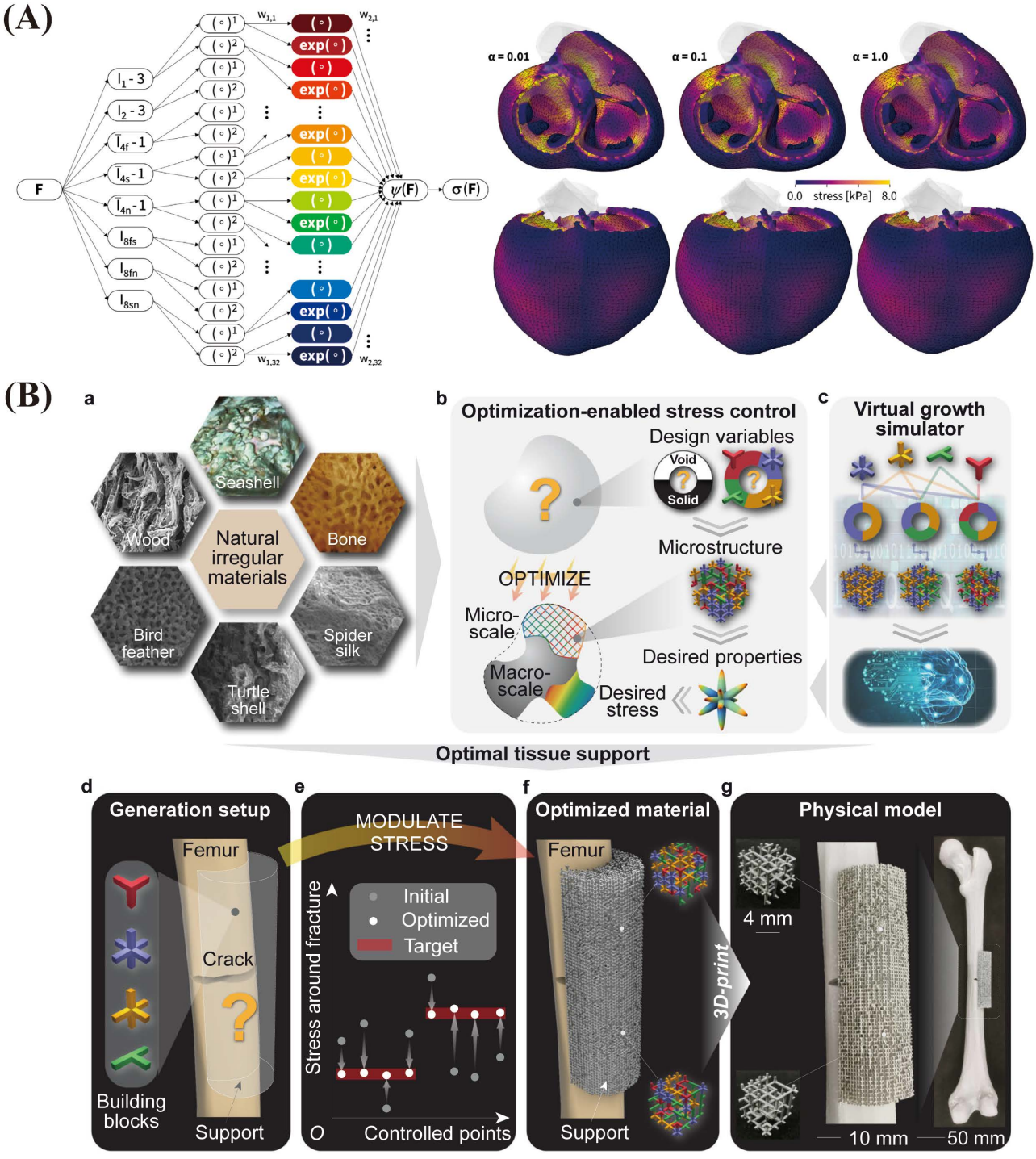

Figure 4. Representative AI-driven modeling and design applications in cardiac and bone tissue engineering. **(A)** Constitutive neural network for human myocardial tissue modeling. The orthotropic, incompressible feedforward network approximates the free energy function from eight

strain invariants across two hidden layers, with polyconvexity enforced by design through selective connectivity. Stress distributions across the human heart under physiological end-diastolic pressures are shown for models discovered at three regularization levels (α = 0.01, 0.1, and 1.0), illustrating the capacity for patient-specific cardiac mechanical characterization [69]; **(B)** Bio-inspired design of irregular architected materials for tissue support. Natural irregular structures provide the basis for the design concept **(a)**. Their local architecture and directional mechanical properties are then optimized according to the desired stress distribution **(b)**. A virtual growth process generates disordered microstructures, while a machine-learning model predicts their material properties for further optimization **(c)**. The framework is applied to a fractured-femur model, in which a support region is defined around the defect **(d)**. The resulting stress distribution is compared with the initial and target conditions **(e)**. This process produces an irregular support structure with spatially varied microstructures **(f)**, which is subsequently **(g)** fabricated by 3D printing at different scales [70]. This figure is licensed under the Creative Commons Attribution 4.0 International License (CC BY 4.0).

A key limitation is that many training datasets rely mainly on numerical simulations. Simulated geometries and boundary conditions may not capture the irregular anatomy, loading, or regeneration of clinical bone defects [71]. Translation also introduces variation from material batches, printing settings, and post-processing. A computed-tomography-based FEM, artificial-neural-network, and Bayesian-network workflow has enabled patient-specific scaffold design within a clinically practical time frame [72]. However, broader use still requires validation across printers, materials, anatomical sites, and patient populations. Integrating micro-CT, patient-specific loading, and longitudinal regeneration data may improve clinical relevance.

4.3. Cartilage tissue engineering scaffolds

Cartilage scaffolds require both load-bearing capacity and low-friction performance. These functions also vary through the depth of articular cartilage, which makes the design of graded constructs particularly challenging. Compared with bone applications, fewer studies have applied generative methods directly to cartilage-scaffold design. Available work has often focused on material selection, graded structural design, or multi-objective optimization.

Literature-mining and multinomial-logistic-regression approaches have been used to identify polymer combinations for cartilage repair [64]. These methods address material selection rather than scaffold architecture, but they can provide inputs for later structural optimization. The Direct MultiSearch framework has also been applied to identify Pareto-optimal TPMS structures that balance mechanical and mass-transport performance. Its reported formulation is applicable to cartilage-differentiation scenarios [65].

Patient-specific manufacturing workflows provide another relevant line of work. An MRI-based workflow was used to design and manufacture a biphasic osteochondral implant with osseous, interlocking, and chondral zones. The construct was fabricated by multichannel three-dimensional extrusion printing using calcium phosphate cement and alginate hydrogel [73]. Although the study did not use a deep generative model, it illustrates a potential workflow linking clinical imaging, computer-aided design, fabrication, and implantation assessment.

Dedicated cartilage datasets remain limited. Public datasets rarely include matched depth-dependent mechanical properties, friction coefficients, permeability, structural features, and biological outcomes [64].

Consequently, many studies remain in silico. Future models should capture functional gradients in cartilage and osteochondral tissue, while experimental validation should assess friction, durability, tissue integration, and cellular outcomes rather than structural similarity alone.

4.4. Other tissue engineering scaffolds

AI-assisted scaffold research is expanding to neural, vascular, and tendon–ligament applications, although progress differs across tissues because their data availability and functional demands vary.

In neural tissue engineering, machine-learning methods have been used to screen materials and optimize nerve-conduit biocompatibility and mechanical behaviour [74]. Direct generation of three-dimensional neural scaffolds remains limited. Vascular scaffolds must maintain lumen patency, mechanical compliance, controlled degradation, and resistance to flow-related stresses. Constrained optimization can incorporate microstructure, mechanical behaviour, and degradation kinetics within the same design process [75].

Tendon and ligament scaffolds must reproduce the gradual transition from soft tissue to bone. Machine-learning models have predicted the effects of braiding parameters on mechanical properties with lower errors than conventional regression in the reported study [76]. Hybrid additive manufacturing and data-driven optimization have also produced constructs with bone-like, enthesis-like, and ligament-like regions [77].

Across these applications, AI is used more often for property prediction and parameter optimization than for direct scaffold generation. Limited datasets and variable fabrication protocols remain major constraints. Progress will require tissue-specific datasets linking scaffold architecture, composition, manufacturing parameters, and biological outcomes. Evaluation should also include endpoints such as neural guidance, vascular patency, and enthesis integration, rather than mechanical performance alone.

5. Current challenges and future directions

Comparing generative scaffold-design studies requires clear reporting of how constraints are incorporated. Biological, mechanical, and manufacturing requirements may be used as conditional inputs, loss penalties, or optimization constraints. These choices shape both the generated designs and their evaluation.

Biological requirements are often represented as conditional variables. For example, a constraint-aware conditional GAN for biofunctional polymer design used cell-viability and proliferation measures to condition pore architecture generation [78]. Similar strategies could incorporate cell-state annotations derived from single-cell or spatial transcriptomic data, provided that the annotations are linked to well-defined scaffold outcomes. This remains difficult because biological responses depend on cell source, culture conditions, material composition, and the time point of measurement.

Mechanical requirements can be included through physics-based or data-driven approaches. Physics-informed neural networks add residuals from governing equations to the training objective. In one study, this approach was used to model material–process–property relationships in extruded GelMA/alginate scaffolds while retaining physical constraints [79]. A second approach uses a surrogate model to associate latent representations with mechanical properties. Regression heads attached to variational autoencoders can predict stiffness-related properties from latent variables and support

gradient-based searches for target mechanical responses [55]. Both approaches are useful, but their reliability depends on the validity of the underlying mechanical model and the quality of the training data.

Manufacturing constraints should be assessed separately from biological and mechanical targets. Overhang angle, minimum feature size, and support requirements determine whether a generated design is printable. Hard constraints exclude non-printable structures, whereas soft constraints penalize poor printability during optimization. Self-supporting constraints have been incorporated into topology-optimization frameworks [60]. More integrated strategies are beginning to appear. TriTopo-LGDM combines topology priors with a diffusion model to account for mechanical targets and printability criteria. In another workflow, GAN-based generation and finite element analysis were combined to balance elastic modulus and yield strength against porosity and specific surface area [62]. These studies illustrate that the location of a constraint in the modelling pipeline should be stated clearly when generative methods are compared.

Despite recent progress, translation to clinical use remains limited by three related issues: data availability, model validation, and manufacturing reproducibility [80,81]. Many published models are trained primarily on simulated datasets. In contrast, patient-specific imaging, physiological loading conditions, and long-term regeneration data are far less available [82]. This mismatch may limit performance when models are applied to real defects. Interpretability and data quality have also been identified as recurring concerns in artificial-intelligence-assisted biomaterials research [83].

Validation remains a major gap. High accuracy on simulated test sets does not show that a scaffold will perform after fabrication or implantation. Mechanical testing, cell culture, and animal studies provide stronger evidence, but remain less common [61]. Validation should match the intended use: cardiac scaffolds require cyclic stability and electrophysiological testing, whereas cartilage scaffolds require assessment of friction, durability, and tissue integration.

Many optimization frameworks also omit tissue-specific functions. In addition to mechanical properties, models may need to include electrical conduction in cardiac constructs, epithelial barrier function, cartilage lubrication, or vascular-graft antithrombogenicity. Comparisons are further limited by the lack of shared datasets, annotations, and evaluation metrics.

Data infrastructure is therefore essential. CWA 18130:2024 provides a standardized scaffold library [84], and ASTM F2150-19 outlines scaffold-characterization guidance [85]. FAIR-compliant libraries can supply additive-manufacturing design files [86], while BioMGE integrates biomaterial and multi-omics data [87]. These resources remain fragmented.

A useful dataset should link scaffold composition, fabrication parameters, and geometry with imaging, mechanical, biological, and degradation data. Relevant measures include micro-CT, scanning electron microscopy, confocal microscopy, stress – strain responses, elastic moduli, cell viability, differentiation, transcriptomic profiles, cytokine responses, and *in vivo* outcomes [88]. Standardized protocols for acquisition and annotation would be necessary before such data could support reliable comparison or model training.

Future work should integrate data, model development, and translation. Biomaterialomics offers one framework for incorporating high-dimensional biological data [89], while physics-informed machine learning, neural ordinary differential equations, and neural operators may help when data are limited or physical constraints are important [90]. These approaches require experimental validation in workflows

linking patient imaging, design, fabrication, bench testing, and *in vivo* assessment. Scalability, reproducibility, and regulatory approval will also be critical for patient-specific scaffolds.

6. Conclusion

Generative AI can expand scaffold design beyond trial-and-error approaches. This review has examined the multimodal data, model families, and tissue-specific requirements that shape inverse design. Imaging, mechanical testing, cellular and molecular measurements, and degradation data provide complementary information, but only when collected and interpreted in compatible ways.

GANs, variational autoencoders, diffusion models, and evolutionary algorithms support different inverse-design tasks. Method selection should reflect the available data, design variables, constraints, and validation strategy. Performance criteria also differ across cardiac, bone, cartilage, vascular, neural, and tendon–ligament applications.

Limited experimental datasets, inconsistent data standards, and insufficient validation remain key barriers. Progress will require datasets linking scaffold architecture, material composition, manufacturing conditions, and biological outcomes, together with validation of fabrication feasibility, mechanical performance, biological response, and tissue-specific function. These steps may support more informed, patient-specific scaffold design.

Declaration of generative AI and AI-assisted technologies

During the preparation of this manuscript, the authors used generative AI tools only to improve language and readability. Specifically, the authors used ChatGPT for language polishing and idea development in limited sections. The authors take full responsibility for the content of the manuscript.

Acknowledgments

We extend our heartfelt appreciation to the anonymous editors and reviewers, whose diligent efforts significantly enhanced the quality of this paper. This study was supported financially by the Student Innovation Ability Enhancement Project–Provincial Level (Grand number: 02-408-240603131021). The graphical abstract was created at https://www.biorender.com/.

Authors' contributions

Conceptualization: H. D., Z.Q., and M.K.; data curation: H.D. and Z.Q.; formal analysis: H.D. and Z.Q.; funding acquisition: M.K.; investigation: H.D., Z.Q., and M.K.; methodology: H.D. and Z.Q.; project administration: M.K.; resources: Z.Q.; software: H.D. and Z.Q.; supervision: M.K.; validation: H.D. and Z.Q.; visualization: H.D. and Z.Q.; writing—original draft: H.D., Z.Q. and M.K.; writing—review and editing: H. D., Z.Q. and M.K. All authors have read and agreed to the published version of the manuscript.

Conflicts of interest

The authors declare that the research was conducted in the absence of any commercial or financial relationships that could be construed as potential conflicts of interest.

Abbreviations

Abbreviations	Full forms
3D CNN	Three-dimensional Convolutional Neural Network
3D-CGAN	Three-dimensional Conditional Generative Adversarial Network
ACL	Anterior Cruciate Ligament
AI	Artificial Intelligence
ANN	Artificial Neural Network
BPNN	Back-Propagation Neural Network
CAD	Computer-Aided Design
CT	Computed Tomography
DDIM	Denoising Diffusion Implicit Model
DDPM	Denoising Diffusion Probabilistic Model
DMA	Dynamic Mechanical Analysis
EA	Evolutionary Algorithm
ECM	Extracellular Matrix
FAIR	Findable, Accessible, Interoperable, and Reusable
FEM	Finite Element Method
GA	Genetic Algorithm
GAN	Generative Adversarial Network
L-BOM	Large-scale Bicontinuous Multiscale structure
LGDM	Latent Graph Diffusion Model
micro-CT	Micro-computed tomography
MG-LDM	Multimodal Guided Latent Diffusion Model
MRI	Magnetic Resonance Imaging
NL-MOD	Nonlinear Machine learning framework for Optimal Design
PCL	Polycaprolactone
PSO	Particle Swarm Optimization
pVAE	property-augmented Variational Autoencoder
RGA	Regenerative Genetic Algorithm
RhoA	Ras Homolog Family Member A
ROCK	Rho-associated Coiled-coil-containing Protein Kinase
scRNA-seq	Single-cell RNA sequencing
scVI	single-cell Variational Inference
SEM	Scanning Electron Microscopy
SLERP	Spherical Linear Interpolation
TAZ	Transcriptional Coactivator with PDZ-binding Motif
TPMS	Triply Periodic Minimal Surface
UMAP	Uniform Manifold Approximation and Projection
VAE	Variational Autoencoder
YAP	Yes-associated protein

References

[1] Valchanov P, Yaneva Y, Pavlov S, Kontny A, Dikova T. The concept of the optimal bioscaffold: parameters, problems, and their resolution through additive manufacturing. *Biomedicines* 2025, 13(11):2688.

[2] Picado-Tejero D, Mendoza-Cerezo L, Rodríguez-Rego JM, Carrasco-Amador JP, Marcos-Romero AC. Recent advances in 3D bioprinting of porous scaffolds for tissue engineering: a narrative and critical review. *J. Funct. Biomater.* 2025, 16(9):328.

[3] Zhou B, Li X, Pan Y, He B, Gao B. Artificial intelligence-assisted next-generation biomaterials: From design and preparation to medical applications. *Colloids Surf. B Biointerfaces* 2025, 255:114970.

[4] Foroughi AH, Valeri C, Razavi MJ. A review of computational optimization of bone scaffold architecture: methods, challenges, and perspectives. *Prog. Biomed. Eng.* 2024, 7(1):012003.

[5] Roldán E, Reeves ND, Cooper G, Andrews K. Machine learning to predict morphology, topography and mechanical properties of sustainable gelatin-based electrospun scaffolds. *Sci. Rep.* 2024, 14(1):21017.

[6] Ahmed E, Mulay P, Ramirez C, Tirado-Mansilla G, Cheong E, *et al.* Mapping biomaterial complexity by machine learning. *Tissue Eng. Part A* 2024, 30(19–20):662–680.

[7] Poltue T, Karuna C, Khrueaduangkham S, Seehanam S, Promoppatum P. Design exploration of 3D-printed triply periodic minimal surface scaffolds for bone implants. *Int. J. Mech. Sci.* 2021, 211:106762.

[8] Zheng X, Chen T, Jiang X, Naito M, Watanabe I. Deep-learning-based inverse design of three-dimensional architected cellular materials with the target porosity and stiffness using voxelized Voronoi lattices. *Sci. Technol. Adv. Mater.* 2023, 24(1):2157682.

[9] Lyu X, Ren X. Microstructure reconstruction of 2D/3D random materials via diffusion-based deep generative models. *Sci. Rep.* 2024, 14(1):5041.

[10] Wang H, Lyu Y, Jiang J, Zhu H. Data-driven inverse design of novel spinodoid bone scaffolds with highly matched mechanical properties in three orthogonal directions. *Mater. Des.* 2025, 251:113697.

[11] Liu W, Zhang Y, Lyu Y, Bosiakov S, Liu Y. Inverse design of anisotropic bone scaffold based on machine learning and regenerative genetic algorithm. *Front. Bioeng. Biotechnol.* 2023, 11:1241151.

[12] Hu J, Wang Y, Tian H, Zheng P, Chi L, *et al.* Intelligent generative design: a transfer learning-enhanced bidirectional mapping framework for customised parametric structural design. *Virtual Phys. Prototyping* 2025, 29(1):e2510001.

[13] Stear BJ, Mohseni Ahooyi T, Simmons JA, Kollar C, Hartman L, *et al.* Petagraph: a large-scale unifying knowledge graph framework for integrating biomolecular and biomedical data. *Sci. Data* 2024, 11(1):1338.

[14] Pan Q, Shen H, Li P, Lai B, Jiang A, *et al.* In silico design of heterogeneous microvascular trees using generative adversarial networks and constrained constructive optimization. *Microcirculation* 2024, 31(5):e12854.

[15] Drakoulas G, Gortsas T, Polyzos E, Tsinopoulos S, Pyl L, *et al.* An explainable machine learning-based probabilistic framework for the design of scaffolds in bone tissue engineering. *Biomech. Model. Mechanobiol.* 2024, 23(3):987–1012.

[16] DePalma SJ, Jilberto J, Stis AE, Huang DD, Lo J, *et al.* Matrix architecture and mechanics regulate myofibril organization, costamere assembly, and contractility in engineered myocardial microtissues. *Adv. Sci.* 2024, 11(47):e2309740.

[17] Sestito JM, Harris TAL, Wang Y. Structural descriptor and surrogate modeling for design of biodegradable scaffolds. *J. Mech. Behav. Biomed. Mater.* 2024, 152:106415.

[18] Yu K, Zhang W, Lu L, Lin Z, Chen B, *et al.* MG-LDM: a multimodal guided latent diffusion model with Mamba-based temporal encoding for inverse topological design of tissue engineering skin substitutes. *Adv. Eng. Inf.* 2025, 71:104275.

[19] Cengiz IF, Oliveira JM, Reis RL. Micro-CT—a digital 3D microstructural voyage into scaffolds: a systematic review of the reported methods and results. *Biomater. Res.* 2018, 22:26.

[20] Cartlidge TAA, Wu Y, Robertson TBR, Katsamenis OL, Pileio G. In silico simulations of diffusion tensors and tortuosity in cells grown on 3D-printed scaffolds for tissue engineering. *RSC Adv.* 2024, 14(44):32398–32410.

[21] Schädli GN, Vetsch JR, Baumann RP, de Leeuw AM, Wehrle E, *et al.* Time-lapsed imaging of nanocomposite scaffolds reveals increased bone formation in dynamic compression bioreactors. *Commun. Biol.* 2021, 4(1):110.

[22] Chen J, Shen S, Xu L, Zheng Z, Zou X, *et al.* Diffusion model-based design of bionic bone scaffolds with tunable microstructures. *Ann. Biomed. Eng.* 2025, 53(12):3285–3301.

[23] Jhuboo R. Super-resolution for bone microstructure CT imaging: morphometry guided super-resolution. Doctoral Thesis, Université Jean Monnet Saint-Étienne, 2024.

[24] Harris N, Zou M. Controlling the organization and differentiation of human neural stem cells on Hilbert microcapillary scaffolds fabricated via two-photon lithography. *Adv. Healthcare Mater.* 2026, 15(2):e01355.

[25] Roldán E, Reeves ND, Cooper G, Andrews K. Machine learning to mechanically assess 2D and 3D biomimetic electrospun scaffolds for tissue engineering applications: between the predictability and the interpretability. *J. Mech. Behav. Biomed. Mater.* 2024, 157:106630.

[26] Puchi-Cabrera ES, Rossi E, Sansonetti G, Sebastiani M, Bemporad E. Machine learning aided nanoindentation: a review of the current state and future perspectives. *Curr. Opin. Solid State Mater. Sci.* 2023, 27(4):101091.

[27] Ibrahimi S, D'Andrea L, Gastaldi D, Rivolta MW, Vena P. Machine learning approaches for the design of biomechanically compatible bone tissue engineering scaffolds. *Comput. Methods Appl. Mech. Eng.* 2024, 423:116842.

[28] Salahshoor H, Ortiz M. Model-free data-driven viscoelasticity in the frequency domain. *Comput. Methods Appl. Mech. Eng.* 2022, 403:115657.

[29] Ruta A, Krishnan K, Elisseeff JH. Single-cell transcriptomics in tissue engineering and regenerative medicine. *Nat. Rev. Bioeng.* 2023, 2:101–119.

[30] Lopez R, Regier J, Cole MB, Jordan MI, Yosef N. Deep generative modeling for single-cell transcriptomics. *Nat. Methods* 2018, 15(12):1053–1058.

[31] Lotfollahi M, Wolf FA, Theis FJ. scGen predicts single-cell perturbation responses. *Nat. Methods* 2019, 16:715–721.

[32] Zinati Y, Takiddeen A, Emad A. GRouNdGAN: GRN-guided simulation of single-cell RNA-seq data using causal generative adversarial networks. *Nat. Commun.* 2024, 15(1):4055.

[33] Gulati GS, D'Silva JP, Liu Y, Wang L, Newman AM. Profiling cell identity and tissue architecture with single-cell and spatial transcriptomics. *Nat. Rev. Mol. Cell Biol.* 2025, 26(1):11–31.

[34] Megas S, Chen DG, Polanski K, Asadollahzadeh H, Eliasof M, *et al.* Celcomen: spatial causal disentanglement for single-cell and tissue perturbation modeling. *Nat. Commun.* 2026, 17(1):4126.

[35] Lou W, Qiu X, Qin Y, Lu Y, Cao Y, *et al.* 3D-printed advanced scaffold armed with exosomes derived from human skeletal stem cell identified by single-cell RNA sequencing enhances osteochondral regeneration. *Bioact. Mater.* 2025, 51:231–256.

[36] Lin P, Qian Z, Liu S, Ye X, Xue P, *et al.* A single-cell RNA sequencing guided multienzymatic hydrogel design for self-regenerative repair in diabetic mandibular defects. *Adv. Mater.* 2024, 36(50):e2410962.

[37] Chen S, Chu C, Wang C, Yang Y, Xu Z, *et al.* Integrated-omics profiling unveils the disparities of host defense to ECM scaffolds during wound healing in aged individuals. *Biomaterials* 2024, 311:122685.

[38] Chan AHP, Hu Y, Pardavi B, Xu X, Grant AJ, *et al.* Developing a single-cell spatial transcriptomics workflow for *in vivo* evaluation of implanted biomaterials. *Adv. Sci.* 2026, 13(24):e13242.

[39] Feng Y, Robers Z, Rasheed L, Miao Y, Wen S, *et al.* MORPHE: bridging image generation and spatial omics for tissue synthesis. *bioRxiv* 2026.

[40] Riasad A, Sayeem Been Z, Wasimul K, Arefin Ittesafun A, Mohaimenul Azam Khan R, *et al.* Generative artificial intelligence in bioinformatics: a systematic review of models, applications, and methodological advances. *arXiv* 2025, arXiv:2511.03354.

[41] Kong Z, Qiu M, Boesen J, Lin X, Yun S, *et al*. SPATIA: multimodal model for prediction and generation of spatial cell phenotypes. *arXiv* 2025, arXiv:2507.04704.

[42] Zhang W, Yu K, Su L, Yao Y, Lu L, *et al.* TriTopo-LGDM: a reverse design method for trabecular bone scaffolds integrating topology optimization and latent graph diffusion models. *Adv. Eng. Inf.* 2025, 71:104269.

[43] Yang X, Huang M, Chen H, Dai J, Chen J, *et al.* Biomaterial-mediated cell atlas: an insight from single-cell and spatial transcriptomics. *Bioact. Mater.* 2025, 54:1–33.

[44] Pardo PS, Danila D, Misra RDK, Boriek AM. Sensing the stiffness: cellular mechano-sensing at the implant interface. *Cells* 2025, 14(14):1101.

[45] Liu Y, Zhou C, Zhang X, Liu W. Chirality hydroxyapatite gradient scaffold drives osteochondral regeneration via YAP/TAZ-mediated mechanotransduction. *Adv. Healthcare Mater.* 2025, 14(22):e2501668.

[46] Bian N, Chu C, Rung S, Huangphattarakul V, Man Y, *et al.* Immunomodulatory biomaterials and emerging analytical techniques for probing the immune micro-environment. *Tissue Eng. Regen. Med.* 2023, 20(1):11–24.

[47] Morrison RA, Sexton J, Zhang L, Dong E, Phillips M, *et al.* Immunotolerant oligomer scaffolds promote regenerative remodeling and improved muscle structure and function after volumetric muscle loss. *Sci. Rep.* 2026, 16(1):12630.

[48] Das R, Karthika S, Bhasarkar J, Bal DK. GA-coupled ANN model for predicting porosity in alginate gel scaffolds. *J. Mech. Behav. Biomed. Mater.* 2023, 148:106204.

[49] Virijević K, Živanović MN, Nikolić D, Milivojević N, Pavić J, *et al.* AI-driven optimization of PCL/PEG electrospun scaffolds for enhanced *in vivo* wound healing. *ACS Appl. Mater. Interfaces* 2024, 16(18):22989–23002.

[50] Hu X, Zhao X, Liu W. Hierarchical sensing framework for polymer degradation monitoring: a physics-constrained reinforcement learning framework for programmable material discovery. *Sensors* 2025, 25(14):4479.

[51] Zhang H, Yang L, Li C, Wu B, Wang W. ScaffoldGAN: synthesis of scaffold materials based on generative adversarial networks. *Comput.-Aided Des.* 2021, 138:103041.

[52] Sadeghkhani A, Bennett B, Babaei M, Rabbani A. A decade of generative adversarial networks for porous material reconstruction. *arXiv* 2026, arXiv:2603.11836.

[53] Barsha FL, Eberle W. An in-depth review and analysis of mode collapse in generative adversarial networks. *Mach. Learn.* 2025, 114:141.

[54] Nguyen PT, Heider Y, Kochmann DM, Aldakheel F. Deep learning-aided inverse design of porous metamaterials. *Comput. Methods Appl. Mech. Eng.* 2025, 449:118499.

[55] Sardeshmukh A, Reddy S, Gautham BP, Bhattacharyya P. Material microstructure design using VAE-regression with multimodal prior. *arXiv* 2024, arXiv:2402.17806.
[56] Baldwin M, Meisel NA, McComb C. Smooth like butter: evaluating multi-lattice transitions in property-augmented latent spaces. *3D Print. Addit. Manuf.* 2025, 12(1):23–35.
[57] Tashkinov M, Pirogova Y, Kononov E, Shalimov A, Silberschmidt VV. Reconstruction of random structures based on generative adversarial networks: statistical variability of mechanical and morphological properties. *Mathematics* 2025, 13:7.
[58] Sordo Z, Chagnon E, Hu Z, Donatelli JJ, Andeer P, *et al.* Synthetic scientific image generation with VAE, GAN, and diffusion model architectures. *J. Imaging* 2025, 11(8):252.
[59] Liu Y, Li A, Sun H, Li S, Chen S. Optimal structural characteristics of bone tissue engineering scaffolds from bionics and PSO-BP-NSGA III integrated algorithm. *Int. J. Bioprint.* 2025, 11(6):451–471.
[60] Wu Z, Xiao R. A topology optimization approach to structure design with self-supporting constraints in additive manufacturing. *J. Comput. Des. Eng.* 2022, 9(2):364–379.
[61] Tartici I, Bartolo P. Fused filament fabrication manufactured biological scaffolds: an investigation of mechanical properties by using the Taguchi method and machine learning techniques. *J. Mech. Behav. Biomed. Mater.* 2026, 173:107215.
[62] Wu X, Zhang F, Huang Y, Wang B, Xinye Y. Multiobjective design of bone scaffolds based on active learning. *J. Mech. Mater. Struct.* 2026, 21(1):29–48.
[63] Jones LS, Rodriguez Cetina Biefer H, Mekkattu M, Thijssen Q, Amicone A, *et al.* Volumetric 3D printing and melt-electrowriting to fabricate implantable reinforced cardiac tissue patches. *Adv. Mater.* 2025, 37(45):e2504765.
[64] Mairpady A, Mourad AI, Mozumder MS. Accelerated discovery of the polymer blends for cartilage repair through data-mining tools and machine-learning algorithm. *Polymers* 2022, 14(9):1802.
[65] Pires THV, Madeira JFA, Castro APG, Fernandes PR. Direct MultiSearch optimization of TPMS scaffolds for bone tissue engineering. *Comput. Methods Programs Biomed.* 2024, 257:108461.
[66] Al Khafaji AT, Barakat AM, Jooda Al Zaidy A, Taan AA, Al-Aouadi RFA. Recent advances in cardiac tissue engineering: innovations and future directions. *Biotechnol. J.* 2025, 20(9):e70116.
[67] Guibert B, Poerio A, Nicole L, Budzinski J, Leroux MM, *et al.* Customizable patterned membranes for cardiac tissue engineering: a model-assisted design method. *J. Mech. Behav. Biomed. Mater.* 2025, 162:106815.
[68] Wu Z, Park J, Steiner PR, Zhu B, Zhang JXJ. Generative adversarial network model to classify human induced pluripotent stem cell-cardiomyocytes based on maturation level. *Sci. Rep.* 2024, 14(1):27016.
[69] Martonová D, Peirlinck M, Linka K, Holzapfel GA, Leyendecker S, *et al.* Automated model discovery for human cardiac tissue: discovering the best model and parameters. *Comput. Methods Appl. Mech. Eng.* 2024, 428:117078.
[70] Jia Y, Liu K, Zhang XS. Modulate stress distribution with bio-inspired irregular architected materials towards optimal tissue support. *Nat. Commun.* 2024, 15(1):4072.
[71] Carlier A, Geris L, Lammens J, Van Oosterwyck H. Bringing computational models of bone regeneration to the clinic. *Wiley Interdiscip. Rev. Syst. Biol. Med.* 2015, 7(4):183–194.

[72] Beisekenov N, Azamatov B, Sadenova M, Dogadkin D, Kaliyev D, *et al.* Data-driven design and additive manufacturing of patient-specific lattice titanium scaffolds for mandibular bone reconstruction. *J. Funct. Biomater.* 2025, 16(9):350.

[73] Von Witzleben M, Liu S, Sembdner P, Holtzhausen S, Blum SFU, *et al.* Additive manufacturing of patient-specific, biphasic implants with zonal design for regeneration of osteochondral defects-critical evaluation of the work flow from clinical MRI data to implantation. *Mater. Today Bio* 2025, 32:101858.

[74] Zhang Z, Yao Y, Wang Z, Bai H, Jiang M, *et al.* Artificial intelligence and peripheral neuropathies: Strategies for the development, application, and repair of regenerative biomaterials. *Neural. Regen. Res.* 2025, 21(9):3952–3963.

[75] Hsu RM, Szafron JM, Carvalho CC, Humphrey JD, Marsden AL. Constrained optimization of scaffold behavior for improving tissue engineered vascular grafts. *J. Biomech.* 2025, 186:112670.

[76] Peng Y, Liu G, Li S, Li Z, Song J. A machine learning system for artificial ligaments with desired mechanical properties in ACL reconstruction applications. *J. Mech. Behav. Biomed. Mater.* 2024, 159:106691.

[77] Micalizzi S, Bevilacqua A, Stefano LD, Gaetano F, Potere F, *et al.* Hybrid additive manufacturing and data-guided design optimization for graded anterior cruciate ligament engineering. *Biomed. Mater.* 2026, 21(1):015013.

[78] Benaatou W, Wani MA, Shakil KA. Deep generative inverse design of biofunctional polymer coatings using conditional GANs. *Digital Discovery* 2026, 5(5):2137–2150.

[79] Yin X, Hao J, Liu S, Lu Y. Hybrid physics-informed and data-driven modeling of material–process–property relationships in extrusion-printed GelMA/alginate vascular scaffolds. *Addit. Manuf.* 2026, 125:105251.

[80] Chakrapani G, Vijay Kumar V, Zare M. Next-generation biomaterials: design strategies, clinical translation, and the rise of intelligent therapeutic platforms. *ACS Omega* 2025, 10(40):46272–46293.

[81] Pugliese R, Badini S, Frontoni E, Regondi S. Generative artificial intelligence for advancing discovery and design in biomateriomics. *Intell. Comput.* 2025, 4:0117.

[82] Wu Y, Ding X, Wang Y, Ouyang D. Harnessing the power of machine learning into tissue engineering: current progress and future prospects. *Burns Trauma* 2024, 12:tkae053.

[83] Ng JC, Yeoh PSQ, Muhamad F, Zhao X, Wu S, *et al.* Advancing biomaterial research with artificial intelligence. *Biomater. Adv* .2026, 180:214535.

[84] European Committee for Standardization (CEN). Standardized scaffolds library for tissue engineering research and industrial applications. 2024. Available: https://www.cencenelec.eu/media/CEN-CENELEC/CWAs/RI/2024/cwa18130.pdf (accessed on 29 June 2026).

[85] International ASTM. ASTM F2150-19 standard guide for characterization and testing of biomaterial scaffolds used in regenerative medicine and tissue-engineered medical products. 2019. Available: https://www.astm.org/f2150-19.html (accessed on 29 June 2026).

[86] Martínez Cendrero A, Franco Martínez F, Solórzano Requejo WG, Díaz Lantada A. Open-source library of tissue engineering scaffolds. *Mater. Des.* 2022, 223:111154.

[87] Gong H, Zhang X, Zhang S, Li M, Zhao H, *et al*. BioMGE: a database for biomedical material and multiomics data collection and analysis. *Chin. J. Eng.* 2024, 46(2):279–289.

[88] Jeznach O, Tabakoglu S, Zaszczyńska A, Sajkiewicz P. Review on machine learning application in tissue engineering: what has been done so far? Application areas, challenges, and perspectives. *J. Mater. Sci.* 2024, 59(46):21222–21250.

[89] Basu B, Gowtham NH, Xiao Y, Kalidindi SR, Leong KW. Biomaterialomics: data science-driven pathways to develop fourth-generation biomaterials. *Acta Biomater.* 2022, 143:1–25.

[90] Ahmadi N, Cao Q, Humphrey JD, Karniadakis GE. Physics-informed machine learning in biomedical science and engineering. *Annu. Rev. Biomed. Eng.* 2026, 28(1):309–336.